


Drive dependence of the Hall angle for a sliding Wigner crystal in a magnetic fieldC. Reichhardt and C. J. O. Reichhardt *Theoretical Division and Center for Nonlinear Studies, Los Alamos National Laboratory, Los Alamos, New Mexico 87545, USA*

(Received 23 November 2020; revised 22 January 2021; accepted 22 February 2021; published 3 March 2021)

We numerically examine the depinning and sliding dynamics of a Wigner crystal in the presence of quenched disorder and a magnetic field. In the disorder-free limit, the Wigner crystal Hall angle is independent of crystal velocity, but when disorder is present, we find that the Hall angle starts near zero at the depinning threshold and increases linearly with increasing drive before reaching a saturation close to the disorder free value at the highest drives. The drive dependence is the result of a side jump effect produced when the charges move over pinning sites. The magnitude of the side jump is reduced at the higher velocities. The drive dependent Hall angle is robust for a wide range of disorder parameters and should be a generic feature of classical charges driven in the presence of quenched disorder and a magnetic field.

DOI: [10.1103/PhysRevB.103.125107](https://doi.org/10.1103/PhysRevB.103.125107)**I. INTRODUCTION**

There are a wide range of systems containing quenched disorder that exhibit depinning and sliding phenomena [1,2], including vortices in type-II superconductors [3,4], driven charge density waves [5,6], skyrmions [7–10], and colloids on substrates [11–13]. Such systems can exhibit a threshold for motion and nonlinear velocity-force curves as a function of increasing external drive. In many cases, the depinning and sliding dynamics can be imaged directly and compared to bulk transport measures, showing that different types of sliding phases are possible including moving crystals and smectic states [2].

A Wigner or electron crystal is also expected to exhibit depinning and sliding under an external drive [14–28]. Experimentally, the presence of nonlinear current-voltage curves or the onset of conduction noise have been argued as providing evidence for the depinning and motion of Wigner crystals [15–19,21–24,28]; however, unlike superconducting vortices or colloidal particles, direct visualization of the depinning process is not possible, so additional transport measures for detecting the sliding of a Wigner crystal would be very valuable. If the sliding Wigner crystal is subjected to a magnetic field, it moves at a Hall angle which is proportional to the strength of the field, but relatively little is known about how the presence of a finite Hall angle could affect depinning or the sliding motion of a Wigner crystal. Based on theoretical calculations in the perturbative limit for a Wigner crystal in a magnetic field interacting with weak quenched disorder, it has been argued that the disorder will not affect the Hall angle [18]; however, it is not clear what happens in the case of strong disorder. In addition to the two-dimensional Wigner crystal systems, one-dimensional or quasi-one-dimensional Wigner crystals can also form [29–32]. There is growing evidence for such states, particularly in carbon nanotubes [33–35]. Both one- and two-dimensional Wigner crystal states should exhibit depinning or sliding under an external drive [36,37].

Depinning and sliding phenomena also appear in magnetic skyrmion systems [7–10], and it has been shown that the skyrmion dynamics are very similar to those of electrons in a magnetic field [7,38]. In particular, the skyrmion motion exhibits a Hall angle with a value that depends on the materials parameters [38]. Simulations of skyrmion motion in the presence of disorder reveal that the skyrmions have a finite depinning threshold and that the skyrmion Hall angle is not constant but has a drive dependence, in which the Hall angle starts near zero at depinning and increases with increasing drive until reaching the disorder free limit at high drives [8,9,38–40]. This effect has now been observed directly in numerous imaging experiments [10,41–45]. Since skyrmions are extended bubblelike objects, the current or disorder can distort the shape or change the size of the skyrmions, potentially generating the drive dependence of the skyrmion Hall angle [41,43,45]. Similar internal distortions could occur in a Wigner crystal. Size distortions do not appear to be required, however, since several simulations using point-like approximations for the skyrmions still found a strong drive dependence of the Hall angle [8,40,46], suggesting that this effect could be generic to other particlelike systems exhibiting a Hall angle in the presence of quenched disorder. In the particle-based skyrmion model, the drive dependence is the result of a velocity-dependent side jump effect, where a particle that passes through a pinning site undergoes a jump in the direction opposite to that of the Hall angle. The jumps are more pronounced at lower velocity [8,47,48]. The presence of such jumps for skyrmions suggests that a similar phenomenon could arise for any particlelike system with a Hall effect, such as a Wigner crystal in a magnetic field, and that the side jumps could be detected by measuring changes in the Hall angle as a function of drive. This would provide an experimentally realizable method for confirming the presence of a sliding Wigner crystal.

We numerically examine a classical model for a Wigner crystal interacting with random disorder using molecular

dynamics simulations. Previous studies of this model in the absence of a magnetic field showed that the system exhibits a depinning threshold and nonlinear current-voltage (I-V) curves [19,23,24]. When a magnetic field is applied, a driven Wigner crystal in a pin-free system moves at a constant Hall angle. If pinning is present, there is a finite depinning threshold and the I-V curves become nonlinear. In addition, the Hall angle develops a strong drive dependence, starting at a value near zero just above depinning and saturating for high drives at a value close to that found in the pin-free or perturbative limit. The drive dependence arises when a charge undergoes a side jump effect upon interacting with the disorder sites. This effect can be confirmed by measurements of the conduction both parallel and perpendicular to the drive. It is predicted to be robust for a wide range of disorder strength and intrinsic Hall angles, and it occurs for both a Wigner crystal and a Wigner glass. The drive-dependent Hall effect provides a method to test for the presence of a Wigner crystal in solid state systems. Our results should also be general to other particlelike charged systems in quenched disorder and could be applied to charged colloids or dusty plasma systems under a magnetic field.

II. SIMULATION AND SYSTEM

We consider the dynamics of a two-dimensional assembly of classical electrons coupled to random pinning using molecular dynamics simulations. In the presence of a magnetic field, the overdamped equation of motion for electron i is given by

$$\alpha_d \mathbf{v}_i = \sum_j^N \nabla U(r_{ij}) + q\mathbf{B} \times \mathbf{v}_i + \mathbf{F}_p + \mathbf{F}_D. \quad (1)$$

Here $U(r) = q/r$ is the repulsive electron-electron interaction potential, q is the electron charge, $q\mathbf{B} \times \mathbf{v}_i$ is the force from the magnetic field which is oriented perpendicular to the electron velocity \mathbf{v}_i , \mathbf{F}_p is the pinning force, \mathbf{F}_D is the force from the externally applied drive, and α_d is the damping term for the velocity component that is aligned with the net external force direction. The system contains N_e electrons and N_{pin} pinning sites. The electron density is given by $\rho = N_e/L^2$ and the pin density is $\rho_p = N_{\text{pin}}/L^2$, where $L = 36$ is the sample size. The pinning is modeled as harmonic traps with a maximum force of F_p and radius r_p . Here we consider the range $F_p = 0.0$ to 0.65 with $r_p = 0.35$. In this system the driving force would arise from an applied voltage or electric field which has a fixed direction. The transition from pinned to sliding would correspond to the onset of conduction, and the Hall angle could be obtained by simultaneously measuring the conduction both parallel and perpendicular to the applied driving field. The Hall angle would be the ratio of the two conduction components. The intrinsic Hall angle could be varied by changing the magnetic field B , while the drive can be varied by changing the voltage. The disorder is quenched, meaning that it is random but fixed in space, and it could be produced by atomic defects, thickness modulations, charge doping, local magnetic defects, and other localized variations in the material. In our case we consider disorder sites that tend to trap electrons, as used in previous simulations [23,24]. There are periodic boundary conditions in the x and y directions, and due to the long range

nature of the electron-electron interactions, we use a Lekner summation technique as in previous studies [23,24].

Previous work with this model was performed in the limit of no magnetic field, $B = 0$, where it was found that when pinning is present, there is a finite depinning threshold for motion, above which the electrons move in the same direction as the external driving force [23,24]. At finite B , the combination of the damping and driving causes the electrons to move at a finite Hall angle θ_H with respect to the driving direction. Since $\theta_H \propto \tan^{-1}(qB/\alpha_d)$, the Hall angle increases with increasing B . For convenience, we measure the magnetic field in units of $B = \alpha_d/q$. We apply a dc driving force $\mathbf{F}_D = F_D \hat{\mathbf{x}}$ and measure the net velocity both parallel and perpendicular to the drive direction, $\langle V_{\parallel} \rangle = N^{-1} \sum_i^N \mathbf{v}_i \cdot \hat{\mathbf{x}}$ and $\langle V_{\perp} \rangle = N^{-1} \sum_i^N \mathbf{v}_i \cdot \hat{\mathbf{y}}$, giving a measured Hall angle of $\theta_{\text{Hall}} = \tan^{-1}(\langle V_{\perp} \rangle / \langle V_{\parallel} \rangle)$.

III. RESULTS

In Fig. 1(a) we show the electrons, pinning sites, and electron trajectories for a system with $F_p = 0.1$, $N_e/N_{\text{pin}} = 0.803$, electron density $\rho = 0.16$, and $B = 0.0$ at $F_D = 0.06$ where the drive is applied in the x direction. A Wigner crystal forms and moves parallel to the driving direction, giving $\theta_{\text{Hall}} = 0.0$. Figure 1(b) shows the same system at a finite magnetic field where the intrinsic or disorder free Hall angle is $\theta_H = \tan^{-1}(qB/\alpha_d) = 26.56^\circ$. Here the Wigner crystal moves at a finite angle of $\theta_{\text{Hall}} = 25^\circ$ which is slightly less than the disorder free θ_H .

In Fig. 2(a) we plot $\langle V_x \rangle$ and $\langle V_y \rangle$ versus F_D for the system in Fig. 1(b), and in Fig. 2(b) we show the corresponding $\theta_{\text{Hall}} = \tan^{-1}(\langle V_y \rangle / \langle V_x \rangle)$ versus F_D . A depinning transition appears near $F_D = 0.0075$, and the nonlinear behavior of the velocity-force curve becomes a linear behavior when $F_D > 0.04$. The dashed line in Fig. 2(b) indicates the pin-free value of θ_H , making it clear that when quenched disorder is present, there is an extended region of drive over which θ_{Hall} increases from zero and then at higher drives begins to saturate to a value close to the pin-free value. In Figs. 2(c) and 2(d) we plot $\langle V_x \rangle$, $\langle V_y \rangle$, and θ_{Hall} versus F_D for a sample with a smaller magnetic field giving $\theta_H = 5.7^\circ$, where we observe the same behavior. We find that for a wide range of θ_H , F_p , and N_{pin} , the general trends illustrated in Fig. 2 persist. Namely, there is a strong drive dependence of the Hall angle for drives up to five times the depinning threshold, followed by a crossover to a saturation regime with a weaker drive dependence.

The velocity dependence of the Hall angle is the result of a side jump effect that occurs as the charges move through the pinning sites. To illustrate this effect, in Fig. 3 we plot the trajectories of a single electron interacting with a pinning site with $F_p = 0.5$. To better highlight the side jumps we use a large intrinsic Hall angle of $\theta_H = 75^\circ$, and we apply the external drive at an angle of -75° from the x axis so that in the absence of pinning the electron motion would be parallel to the x axis. For $F_D = 0.2$ the electron is trapped by the pinning site and undergoes a spiraling motion to reach the minimum energy position of the tilted pin, as shown in Fig. 3(a). For drives that are large enough to permit the electron to escape the trap, the electron trajectory is bowed across the pinning site and the point of exit of the electron is shifted in the

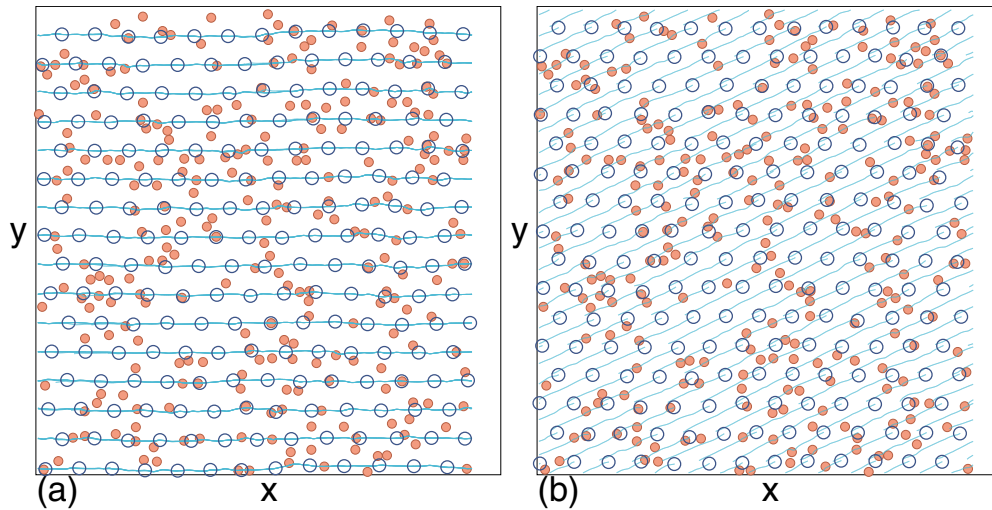


FIG. 1. Images of the Wigner crystal system showing the electrons (blue open circles), pinning sites (orange filled circles), and electron trajectories over a period of time (light blue lines). The driving force $F_D = 0.06$ is applied along the x direction in both cases and the pinning strength is $F_p = 0.1$. (a) At zero magnetic field, $B = 0$, the Hall angle $\theta_{\text{Hall}} = 0$. (b) For a finite magnetic field of $B = 0.5$ where the intrinsic Hall angle is $\theta_H = 26.56^\circ$, the Wigner crystal moves along a direction close to that of the Hall angle.

negative y direction compared to the point of entry. Figure 3(b) illustrates this effect for $F_D = 0.275, 0.3, 0.4, 0.5, 0.7, 1.0$, and 1.5 , where the shift or jump gradually decreases in size with increasing F_D . The side jumps are in the direction opposite to the Hall angle, so that for repeated interactions with pinning sites, the overall average electron motion is at an angle that is smaller than the intrinsic Hall angle θ_H . As the velocity of the electron increases, its direction of motion approaches θ_H .

In Fig. 4(a) we plot a dynamic phase diagram as a function of F_D versus electron density ρ for the system in Figs. 2(c) and 2(d) at fixed pinning density $\rho_p = 0.2$ for $\theta_H = 5.7^\circ$. The pinned state is defined as the regime in which both velocity

components are zero. In the flowing state, the Wigner crystal moves nearly along the intrinsic Hall angle direction, and we define the transition into this state to occur when the measured Hall angle is at least 90% as large as the intrinsic Hall angle. We also mark the regime in which the Hall angle increases linearly with drive, and the region where the crystal is moving but the Hall angle is zero. The latter regime is likely the result of a transverse barrier to motion. Such a transverse pinning effect can also arise in the absence of a magnetic field, as was proposed by Giamarchi and Le Doussal [49,50] for vortices and other particle-like objects moving over random disorder, where the system forms one-dimensional moving channels. Previous numerical studies on sliding Wigner crystals in the

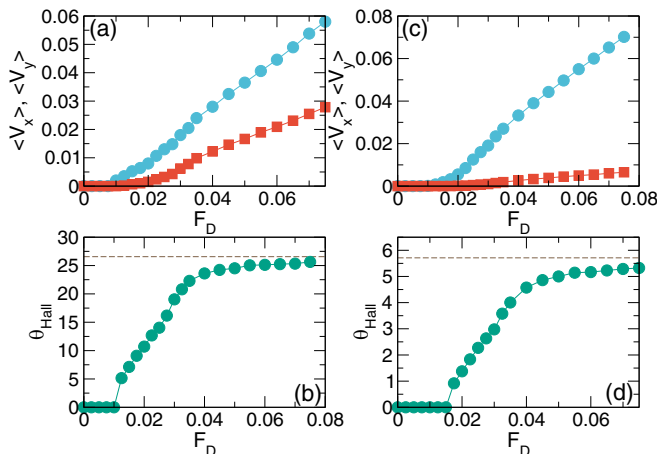


FIG. 2. (a) The x and y velocities $\langle V_x \rangle$ (blue circles) and $\langle V_y \rangle$ (red squares) vs F_D for the system in Fig. 1(b) with $F_p = 0.1$ and $B = 0.5$. (b) The corresponding Hall angle $\theta_{\text{Hall}} = \tan^{-1}(\langle V_y \rangle / \langle V_x \rangle)$. The dashed line indicates the disorder free value of $\theta_H = 26.56^\circ$. (c) $\langle V_x \rangle$, $\langle V_y \rangle$ and (d) θ_{Hall} vs F_D for a system with a smaller magnetic field of $B = 0.1$ which gives $\theta_H = 5.7^\circ$. Here there is a low drive regime where the Hall angle increases linearly with F_D and a higher drive regime where the increase in θ_{Hall} with drive is much slower.

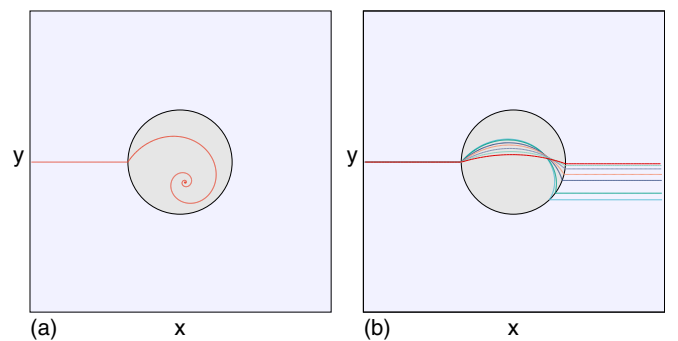


FIG. 3. An electron interacting with an attractive pinning well that has $F_p = 0.5$. Here the intrinsic Hall angle is $\theta_H = 75^\circ$ and the external drive is applied at an angle of -75° to the x axis such that, in the pin-free limit, the electron moves parallel to the x axis. (a) At $F_D = 0.2$, the electron becomes trapped in the pin. (b) $F_D = 0.275$ (light blue), 0.3 (dark green), 0.4 (dark blue), 0.5 (orange), 0.7 (light purple), 1.0 (light green), and 1.5 (red) showing the evolution of the side jump as the electron passes across the pinning site for drives above the depinning threshold. The side jump is in the direction opposite to the Hall angle, and the size of the side jump decreases as the driving force increases.

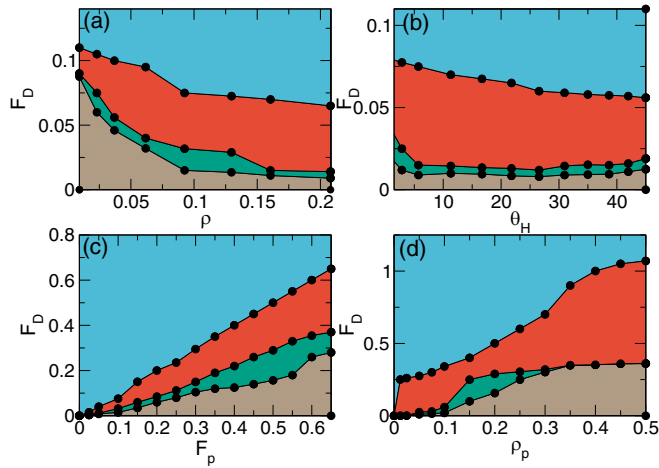


FIG. 4. (a) Dynamic phase diagram as a function of F_D vs electron density ρ for the system in Fig. 2 with $F_p = 0.1$, pin density $\rho_p = 0.2$, and $B = 0.1$, where the intrinsic Hall angle is $\theta_H = 5.7^\circ$. Colors indicate the pinned regime (brown), the flowing saturated regime (blue), the linearly increasing Hall angle regime (orange) and the sliding but zero Hall angle state (green). (b) Dynamic phase diagram as a function of F_D vs intrinsic Hall angle θ_H for the same system at fixed $\rho = 0.16$. (c) Dynamic phase diagram as a function of F_D vs pinning strength F_p for a system with $\rho = 0.0926$, $\rho_p = 0.2$, and $\theta_H = 5.7^\circ$. (d) Dynamic phase diagram as a function of F_D vs pinning density ρ_p for a sample with $\theta_H = 5.7^\circ$, $\rho = 0.0926$, and $F_p = 0.5$.

absence of a magnetic field also found a transverse barrier for motion when an additional driving force was applied transverse to the sliding direction [23]. Although the pinning is random, spatial symmetry breaking occurs due to the Wigner crystalline structure. Once the system is moving, the fluctuations induced in the crystal by the underlying disorder are anisotropic and are strongest in the direction of motion. As a result, the crystal forms what is effectively a series of one-dimensional moving channels, where fluctuations in the channels are the result of the electrons finding the easiest flow path. After these channels form, they create a transverse barrier to motion induced by an external drive applied perpendicular to the channels. Giamarchi and Le Doussal [49,50] proposed that any systems forming a crystalline structure moving over random disorder will show a transverse depinning barrier. Such effects have been studied for superconducting vortex lattices moving over random disorder in the absence of a magnus force [51–53]. Other works on smectic states moving over quenched disorder also predicted a transverse barrier to motion [54]. The novel aspect of the system that we consider here is that no external transverse driving force is applied. Instead, the magnus force acts as an effective additional applied transverse drive due to the finite Hall angle. If the pinning is not random but is instead periodic, the transverse barrier becomes even stronger and a series of steps can appear in the transverse response. Such effects were proposed for electrons moving over periodic scattering arrays [55] and for skyrmion motion in periodic arrays [48].

In Fig. 4(a), for $\rho < 0.075$, the system forms a pinned Wigner glass rather than a pinned Wigner crystal, resulting in an increase in the depinning threshold with decreasing

ρ . Figure 4(b) shows a dynamic phase diagram as a function of F_D versus the intrinsic Hall angle θ_H over the range $\theta_H = 2.86^\circ$ to 45° for the same system at fixed $\rho = 0.16$. In Fig. 4(c) we display the dynamic phase diagram as a function of F_D versus pinning strength F_p for a system with $\theta_H = 5.7^\circ$ and $\rho = 0.0926$, while in Fig. 4(d) we plot a dynamic phase diagram as a function of F_D versus pinning density ρ_p for a system with fixed $\rho = 0.0926$, $F_p = 0.5$, and $\theta_H = 5.7^\circ$. These results indicate that the dynamic phases we observe are robust over a wide range of parameters.

IV. DISCUSSION

Experimentally, the drive dependence of the Hall angle could be detected by measuring the transport above a depinning threshold in a system where a Wigner crystal is expected to form in the presence of a magnetic field. One possible method for measuring both velocity components accurately for varied drives is by creating a cross-shaped geometry of contacts similar to that used for simultaneously detecting the transverse and longitudinal velocity components of moving superconducting vortices [56–59]. An experimental protocol could consist of entering a regime in which a Wigner crystal is expected to be present and performing a series of experiments in which the driving force is swept for selected fixed values of the external magnetic field B , where different choices of B give different values of the Hall angle. It could also be possible to change the effective pinning in the system by introducing periodic arrays of artificial defects, similar to the controlled pinning used in superconducting vortex [60–62] and skyrmion systems [63,64], or by irradiating the sample [65,66].

The drive dependence should be the most pronounced for large magnetic fields. There have already been some limited experimental studies of Wigner crystal sliding in a magnetic field which show that there is a minimum threshold longitudinal velocity which must be exceeded before sliding begins to occur in the transverse direction [67]. Other systems in which a similar effect could appear include a sliding quantum crystal [68,69], creep motion of a Wigner crystal near melting [27,70], or driven electron liquid crystal states [71–73]. In some regimes in these systems, the particle picture breaks down, and in these regimes, the drive dependence of the Hall effect could be absent. Additionally, a similar drive dependent Hall effect should occur for charged colloids or dusty plasmas driven in the presence of quenched disorder and a magnetic field.

V. SUMMARY

We have examined the depinning and sliding of a Wigner crystal in the presence of a magnetic field where in the absence of disorder the crystal moves at a Hall angle that is independent of the crystal velocity. When disorder is present, we find a pinned phase at low drive as well as a sliding phase in which the Hall angle is not constant but is initially zero near the depinning threshold and gradually increases with increasing drive until at high drives it reaches a saturation value close to the intrinsic Hall angle. This effect is the result of the side jump that occurs when the electrons move over the pinning sites, where the jump is in the direction opposite to the Hall angle. The magnitude of the side jump decreases with

increasing velocity, which is similar to the behavior of the side jump effect observed for skyrmions driven over quenched disorder. We also find a regime in which the electrons slide only along the direction of drive and exhibit a finite barrier to transverse motion. The drive dependence of the Hall angle is robust over a wide range of intrinsic Hall angles, disorder densities, and pinning strengths, and could serve as a way to confirm the existence of a sliding Wigner crystal. Our results should be general to the broad class of driven systems with a Hall angle in the presence of disorder.

ACKNOWLEDGMENTS

We gratefully acknowledge the support of the U.S. Department of Energy through the LANL/LDRD program for this work. This work was supported by the U.S. Department of Energy through the Los Alamos National Laboratory. Los Alamos National Laboratory is operated by Triad National Security, LLC, for the National Nuclear Security Administration of the U.S. Department of Energy (Contract No. 892333218NCA000001).

-
- [1] D. S. Fisher, Collective transport in random media: From superconductors to earthquakes, *Phys. Rep.* **301**, 113 (1998).
- [2] C. Reichhardt and C. J. O. Reichhardt, Depinning and nonequilibrium dynamic phases of particle assemblies driven over random and ordered substrates: A review, *Rep. Prog. Phys.* **80**, 026501 (2017).
- [3] S. Bhattacharya and M. J. Higgins, Dynamics of a Disordered Flux Line Lattice, *Phys. Rev. Lett.* **70**, 2617 (1993).
- [4] G. Blatter, M. V. Feigel'man, V. B. Geshkenbein, A. I. Larkin, and V. M. Vinokur, Vortices in high-temperature superconductors, *Rev. Mod. Phys.* **66**, 1125 (1994).
- [5] G. Grüner, The dynamics of charge-density waves, *Rev. Mod. Phys.* **60**, 1129 (1988).
- [6] R. Danneau, A. Ayari, D. Rideau, H. Requardt, J. E. Lorenzo, L. Ortega, P. Monceau, R. Currat, and G. Grübel, Motional Ordering of a Charge-Density Wave in the Sliding State, *Phys. Rev. Lett.* **89**, 106404 (2002).
- [7] T. Schulz, R. Ritz, A. Bauer, M. Halder, M. Wagner, C. Franz, C. Pfeleiderer, K. Everschor, M. Garst, and A. Rosch, Emergent electrodynamics of skyrmions in a chiral magnet, *Nat. Phys.* **8**, 301 (2012).
- [8] C. Reichhardt, D. Ray, and C. J. Olson Reichhardt, Collective Transport Properties of Driven Skyrmions with Random Disorder, *Phys. Rev. Lett.* **114**, 217202 (2015).
- [9] W. Legrand, D. Maccariello, N. Reyren, K. Garcia, C. Moutafis, C. Moreau-Luchaire, S. Coffin, K. Bouzehouane, V. Cros, and A. Fert, Room-temperature current-induced generation and motion of sub-100 nm skyrmions, *Nano Lett.* **17**, 2703 (2017).
- [10] W. Jiang, X. Zhang, G. Yu, W. Zhang, X. Wang, M. B. Jungfleisch, J. E. Pearson, X. Cheng, O. Heinonen, K. L. Wang, Y. Zhou, A. Hoffmann, and S. G. E. te Velthuis, Direct observation of the skyrmion Hall effect, *Nat. Phys.* **13**, 162 (2017).
- [11] C. Reichhardt and C. J. Olson, Colloidal Dynamics on Disordered Substrates, *Phys. Rev. Lett.* **89**, 078301 (2002).
- [12] A. Pertsinidis and X. S. Ling, Statics and Dynamics of 2D Colloidal Crystals in a Random Pinning Potential, *Phys. Rev. Lett.* **100**, 028303 (2008).
- [13] T. Bohlein, J. Mikhael, and C. Bechinger, Observation of kinks and antikinks in colloidal monolayers driven across ordered surfaces, *Nat. Mater.* **11**, 126 (2012).
- [14] E. Y. Andrei, G. Deville, D. C. Glatli, F. I. B. Williams, E. Paris, and B. Etienne, Observation of a Magnetically Induced Wigner Solid, *Phys. Rev. Lett.* **60**, 2765 (1988).
- [15] V. J. Goldman, M. Santos, M. Shayegan, and J. E. Cunningham, Evidence for Two-Dimensional Quantum Wigner Crystal, *Phys. Rev. Lett.* **65**, 2189 (1990).
- [16] F. I. B. Williams, P. A. Wright, R. G. Clark, E. Y. Andrei, G. Deville, D. C. Glatli, O. Probst, B. Etienne, C. Dorin, C. T. Foxon, and J. J. Harris, Conduction Threshold and Pinning Frequency of Magnetically Induced Wigner Solid, *Phys. Rev. Lett.* **66**, 3285 (1991).
- [17] H. W. Jiang, H. L. Stormer, D. C. Tsui, L. N. Pfeiffer, and K. W. West, Magnetotransport studies of the insulating phase around $\nu = 1/5$ Landau-level filling, *Phys. Rev. B* **44**, 8107 (1991).
- [18] X. Zhu, P. B. Littlewood, and A. J. Millis, Sliding motion of a two-dimensional Wigner crystal in a strong magnetic field, *Phys. Rev. B* **50**, 4600 (1994).
- [19] M.-C. Cha and H. A. Fertig, Orientational Order and Depinning of the Disordered Electron Solid, *Phys. Rev. Lett.* **73**, 870 (1994).
- [20] R. Chitra, T. Giamarchi, and P. Le Doussal, Dynamical Properties of the Pinned Wigner Crystal, *Phys. Rev. Lett.* **80**, 3827 (1998).
- [21] F. Perruchot, C. J. Mellor, R. Gaál, B. Sas, G. Deville, B. Etienne, B. L. Gallagher, M. Henini, C. T. Foxon, J. J. Harris, and F. I. B. Williams, Hall effect of pinned and depinned 2-D electron and hole solids, *Physica B* **256-258**, 587 (1998).
- [22] E. Abrahams, S. V. Kravchenko, and M. P. Sarachik, Metallic behavior and related phenomena in two dimensions, *Rev. Mod. Phys.* **73**, 251 (2001).
- [23] C. Reichhardt, C. J. Olson, N. Grønbech-Jensen, and F. Nori, Moving Wigner Glasses and Smectics: Dynamics of Disordered Wigner Crystals, *Phys. Rev. Lett.* **86**, 4354 (2001).
- [24] C. Reichhardt and C. J. Olson Reichhardt, Noise at the Crossover from Wigner Liquid to Wigner Glass, *Phys. Rev. Lett.* **93**, 176405 (2004).
- [25] D. Zhang, X. Huang, W. Dietsche, K. von Klitzing, and J. H. Smet, Signatures for Wigner Crystal Formation in the Chemical Potential of a Two-Dimensional Electron System, *Phys. Rev. Lett.* **113**, 076804 (2014).
- [26] J. Jang, B. M. Hunt, L. N. Pfeiffer, K. W. West, and R. C. Ashoori, Sharp tunneling resonance from the vibrations of an electronic Wigner crystal, *Nat. Phys.* **13**, 340 (2017).
- [27] T. Knighton, Z. Wu, J. Huang, A. Serafin, J. S. Xia, L. N. Pfeiffer, and K. W. West, Evidence of two-stage melting of Wigner solids, *Phys. Rev. B* **97**, 085135 (2018).
- [28] P. Brussarski, S. Li, S. V. Kravchenko, A. A. Shashkin, and M. P. Sarachik, Transport evidence for a sliding two-dimensional quantum electron solid, *Nat. Commun.* **9**, 3803 (2018).
- [29] H. J. Schulz, Wigner Crystal in One Dimension, *Phys. Rev. Lett.* **71**, 1864 (1993).

- [30] K. A. Matveev, Conductance of a Quantum wire in the Wigner-Crystal Regime, *Phys. Rev. Lett.* **92**, 106801 (2004).
- [31] M. Yamamoto, M. Stopa, Y. Tokura, Y. Hirayama, and S. Tarucha, Negative Coulomb drag in a one-dimensional wire, *Science* **313**, 204 (2006).
- [32] N. T. Ziani, F. Cavaliere, K. G. Becerra, and M. Sasseti, A short review of one-dimensional Wigner crystallization, *Crystals* **11**, 20 (2021).
- [33] V. V. Deshpande and M. Bockrath, The one-dimensional Wigner crystal in carbon nanotubes, *Nat. Phys.* **4**, 314 (2008).
- [34] L. Sárkány, E. Szirmai, C. P. Moca, L. Glazman, and G. Zaránd, Wigner crystal phases in confined carbon nanotubes, *Phys. Rev. B* **95**, 115433 (2017).
- [35] I. Shapir, A. Hamo, S. Pecker, C. P. Moca, Ö. Legeza, G. Zarand, and S. Ilani, Imaging the electronic Wigner crystal in one dimension, *Science* **364**, 870 (2019).
- [36] C. Reichhardt and C. J. O. Olson-Reichhardt, Dynamically induced locking and unlocking transitions in driven layered systems with quenched disorder, *Phys. Rev. B* **84**, 174208 (2011).
- [37] S. N. Artemenko, D. S. Shapiro, R. R. Vakhitov, and S. V. Remizov, Sliding regime of conduction in 'one-dimensional Wigner crystal,' *Physica B* **407**, 1894 (2012).
- [38] N. Nagaosa and Y. Tokura, Topological properties and dynamics of magnetic skyrmions, *Nat. Nanotechnol.* **8**, 899 (2013).
- [39] J.-V. Kim and M.-W. Yoo, Current-driven skyrmion dynamics in disordered films, *Appl. Phys. Lett.* **110**, 132404 (2017).
- [40] S. A. Díaz, C. J. O. Reichhardt, D. P. Arovas, A. Saxena, and C. Reichhardt, Fluctuations and noise signatures of driven magnetic skyrmions, *Phys. Rev. B* **96**, 085106 (2017).
- [41] K. Litzius, I. Lemesch, B. Krüger, P. Bassirian, L. Caretta, K. Richter, F. Büttner, K. Sato, O. A. Tretiakov, J. Förster, R. M. Reeve, M. Weigand, L. Bykova, H. Stoll, G. Schütz, G. S. D. Beach, and M. Kläui, Skyrmion Hall effect revealed by direct time-resolved X-ray microscopy, *Nat. Phys.* **13**, 170 (2017).
- [42] S. Woo, K. M. Song, X. Zhang, Y. Zhou, M. Ezawa, X. Liu, S. Finizio, J. Raabe, N. J. Lee, S. Kim, S.-Y. Park, Y. Kim, J.-Y. Kim, D. Lee, O. Lee, J. W. Choi, B.-C. Min, H. C. Koo, and J. Chang, Current-driven dynamics and inhibition of the skyrmion Hall effect of ferrimagnetic skyrmions in GdFeCo films, *Nat. Commun.* **9**, 959 (2018).
- [43] R. Juge, S.-G. Je, D. S. Chaves, L. D. Buda-Prejbeanu, J. Peña Garcia, J. Nath, I. M. Miron, K. G. Rana, L. Aballe, M. Foerster, F. Genuzio, T. O. Menteş, A. Locatelli, F. Maccherozzi, S. S. Dhesi, M. Belmeguenai, Y. Roussigné, S. Auffret, S. Pizzini, G. Gaudin *et al.*, Current-driven skyrmion dynamics and drive-dependent skyrmion Hall effect in an ultrathin film, *Phys. Rev. Appl.* **12**, 044007 (2019).
- [44] K. Zeissler, S. Finizio, C. Barton, A. J. Huxtable, J. Massey, J. Raabe, A. V. Sadovnikov, S. A. Nikitov, R. Brearton, T. Hesjedal, G. van der Laan, M. C. Rosamond, E. H. Linfield, G. Burnell, and C. H. Marrows, Diameter-independent skyrmion Hall angle observed in chiral magnetic multilayers, *Nat. Commun.* **11**, 428 (2020).
- [45] K. Litzius, J. Leliaert, P. Bassirian, D. Rodrigues, S. Kromin, I. Lemesch, J. Zazvorka, K.-J. Lee, J. Mulkers, N. Kerber, D. Heinze, N. Keil, R. M. Reeve, M. Weigand, B. Van Waeyenberge, G. Schütz, K. Everschor-Sitte, G. S. D. Beach, and M. Kläui, The role of temperature and drive current in skyrmion dynamics, *Nat. Electron.* **3**, 30 (2020).
- [46] X. Gong, H. Y. Yuan, and X. R. Wang, Current-driven skyrmion motion in granular films, *Phys. Rev. B* **101**, 064421 (2020).
- [47] J. Müller and A. Rosch, Capturing of a magnetic skyrmion with a hole, *Phys. Rev. B* **91**, 054410 (2015).
- [48] C. Reichhardt, D. Ray, and C. J. O. Reichhardt, Quantized transport for a skyrmion moving on a two-dimensional periodic substrate, *Phys. Rev. B* **91**, 104426 (2015).
- [49] T. Giamarchi and P. Le Doussal, Moving Glass Phase of Driven Lattices, *Phys. Rev. Lett.* **76**, 3408 (1996).
- [50] P. Le Doussal and T. Giamarchi, Moving glass theory of driven lattices with disorder, *Phys. Rev. B* **57**, 11356 (1998).
- [51] K. Moon, R. T. Scalettar, and G. T. Zimányi, Dynamical Phases of Driven Vortex Systems, *Phys. Rev. Lett.* **77**, 2778 (1996).
- [52] C. J. Olson and C. Reichhardt, Transverse depinning in strongly driven vortex lattices with disorder, *Phys. Rev. B* **61**, R3811(R) (2000).
- [53] H. Fangohr, P. A. J. de Groot, and S. J. Cox, Critical transverse forces in weakly pinned driven vortex systems, *Phys. Rev. B* **63**, 064501 (2001).
- [54] L. Balents, M. C. Marchetti, and L. Radzihovsky, Nonequilibrium steady states of driven periodic media, *Phys. Rev. B* **57**, 7705 (1998).
- [55] J. Wiersig and K.-H. Ahn, Devil's Staircase in the Magnetoresistance of a Periodic Array of Scatterers, *Phys. Rev. Lett.* **87**, 026803 (2001).
- [56] A. V. Silhanek, L. Van Look, S. Raedts, R. Jonckheere, and V. V. Moshchalkov, Guided vortex motion in superconductors with a square antidot array, *Phys. Rev. B* **68**, 214504 (2003).
- [57] J. E. Villegas, E. M. Gonzalez, M. I. Montero, I. K. Schuller, and J. L. Vicent, Vortex-lattice dynamics with channeled pinning potential landscapes, *Phys. Rev. B* **72**, 064507 (2005).
- [58] C. J. O. Reichhardt and C. Reichhardt, Coherent and incoherent vortex flow states in crossed channels, *EPL* **88**, 47004 (2009).
- [59] G. Zechner, W. Lang, M. Dosmailov, M. A. Bodea, and J. D. Pedarnig, Transverse vortex commensurability effect and sign change of the hall voltage in superconducting $\text{YBa}_2\text{Cu}_3\text{O}_{7-\delta}$ thin films with a nanoscale periodic pinning landscape, *Phys. Rev. B* **98**, 104508 (2018).
- [60] M. Baert, V. V. Metlushko, R. Jonckheere, V. V. Moshchalkov, and Y. Bruynseraede, Composite Flux-Line Lattices Stabilized in Superconducting Films by a Regular Array of Artificial Defects, *Phys. Rev. Lett.* **74**, 3269 (1995).
- [61] J. I. Martín, M. Vélez, J. Nogués, and I. K. Schuller, Flux Pinning in a Superconductor by an Array of Submicrometer Magnetic Dots, *Phys. Rev. Lett.* **79**, 1929 (1997).
- [62] C. Reichhardt, G. T. Zimányi, and N. Grønbech-Jensen, Complex dynamical flow phases and pinning in superconductors with rectangular pinning arrays, *Phys. Rev. B* **64**, 014501 (2001).
- [63] C. Reichhardt, D. Ray, and C. J. O. Reichhardt, Nonequilibrium phases and segregation for skyrmions on periodic pinning arrays, *Phys. Rev. B* **98**, 134418 (2018).
- [64] J. Feilhauer, S. Saha, J. Tobik, M. Zelent, L. J. Heyderman, and M. Mruczkiewicz, Controlled motion of skyrmions in a magnetic antidot lattice, *Phys. Rev. B* **102**, 184425 (2020).
- [65] L. Civale, A. D. Marwick, T. K. Worthington, M. A. Kirk, J. R. Thompson, L. Krusin-Elbaum, Y. Sun, J. R. Clem, and F. Holtzberg, Vortex Confinement by Columnar Defects in $\text{YBa}_2\text{Cu}_3\text{O}_7$ Crystals: Enhanced Pinning at High Fields and Temperatures, *Phys. Rev. Lett.* **67**, 648 (1991).

- [66] B. Aichner, B. Müller, M. Karrer, V. R. Misko, F. Limberger, K. L. Mletschnig, M. Dosmailov, J. D. Pedarnig, F. Nori, R. Kleiner, D. Koelle, and W. Lang, Ultradense tailored vortex pinning arrays in superconducting $\text{YBa}_2\text{Cu}_3\text{O}_{7-\delta}$ thin films created by focused He ion beam irradiation for fluxonics applications, *ACS Appl. Nano Mater.* **2**, 5108 (2019).
- [67] F. Perruchot, F. I. B. Williams, C. J. Mellor, R. Gaal, B. Sas, and M. Henini, Transverse threshold for sliding conduction in a magnetically induced Wigner solid, *Physica B* **284**, 1984 (2000).
- [68] Y. P. Chen, G. Sambandamurthy, Z. H. Wang, R. M. Lewis, L. W. Engel, D. C. Tsui, P. D. Ye, L. N. Pfeiffer, and K. W. West, Melting of a 2D quantum electron solid in high magnetic field, *Nat. Phys.* **2**, 452 (2006).
- [69] A. A. Shashkin and S. V. Kravchenko, Recent developments in the field of the metal-insulator transition in two dimensions, *Appl. Sci.* **9**, 1169 (2019).
- [70] M. K. Ma, K. A. Villegas Rosales, H. Deng, Y. J. Chung, L. N. Pfeiffer, K. W. West, K. W. Baldwin, R. Winkler, and M. Shayegan, Thermal and Quantum Melting Phase Diagrams for a Magnetic-Field-Induced Wigner Solid, *Phys. Rev. Lett.* **125**, 036601 (2020).
- [71] K. B. Cooper, M. P. Lilly, J. P. Eisenstein, L. N. Pfeiffer, and K. W. West, Insulating phases of two-dimensional electrons in high Landau levels: Observation of sharp thresholds to conduction, *Phys. Rev. B* **60**, R11285(R) (1999).
- [72] C. Reichhardt, C. J. O. Reichhardt, I. Martin, and A. R. Bishop, Dynamical Ordering of Driven Stripe Phases in Quenched Disorder, *Phys. Rev. Lett.* **90**, 026401 (2003).
- [73] X. Wang, H. Fu, L. Du, X. Liu, P. Wang, L. N. Pfeiffer, K. W. West, R.-R. Du, and X. Lin, Depinning transition of bubble phases in a high Landau level, *Phys. Rev. B* **91**, 115301 (2015).